

LTOS: Layout-controllable Text-Object Synthesis via Adaptive Cross-attention Fusions

Xiaoran Zhao
National University of Defense
Technology
China

Tianhao Wu
Nanyang Technological University
Singapore

Yu Lai
National University of Defense
Technology
China

Zhiliang Tian
National University of Defense
Technology
China

Zhen Huang
National University of Defense
Technology
China

Yahui Liu
Huawei Technologies Ltd
China

Zejiang He
National University of Defense
Technology
China

Dongsheng Li
National University of Defense
Technology
China

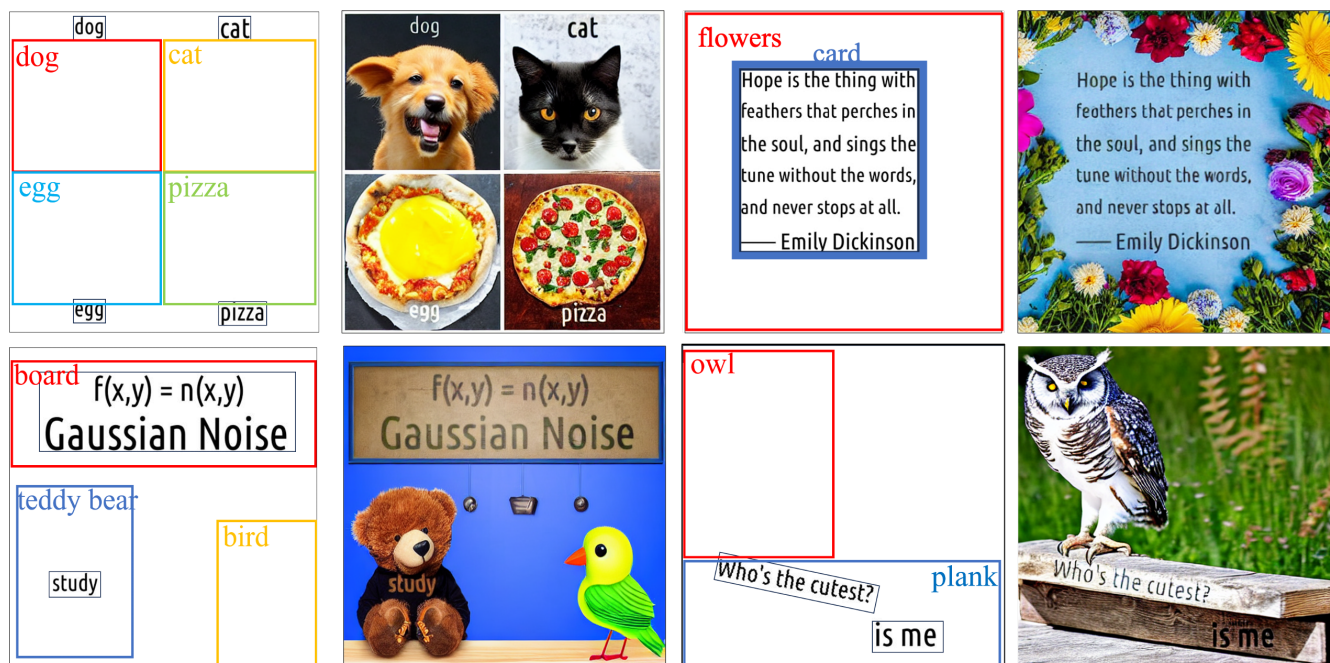


Figure 1: Example results of our TOF model. Given predefined visual text and object information, TOF achieves accurate object generation following the layout map while rendering legible text consistent to the depth, texture, and geometry of the image.

ABSTRACT

Controllable text-to-image generation synthesizes visual text and objects in images with certain conditions, which are frequently applied to emoji and poster generation. Visual text rendering and layout-to-image generation tasks have been popular in controllable text-to-image generation. However, each of these tasks typically focuses on single modality generation or rendering, leaving yet-to-be-bridged gaps between the approaches correspondingly designed for each of the tasks. In this paper, we combine text rendering and layout-to-image generation tasks into a single task:

layout-controllable text-object synthesis (LTOS) task, aiming at synthesizing images with object and visual text based on predefined object layout and text contents. As compliant datasets are not readily available for our LTOS task, we construct a layout-aware text-object synthesis dataset, containing elaborate well-aligned labels of visual text and object information. Based on the dataset, we propose a layout-controllable text-object adaptive fusion (TOF) framework, which generates images with clear, legible visual text and plausible objects. We construct a visual-text rendering module to synthesize text and employ an object-layout control module

to generate objects while integrating the two modules to harmoniously generate and integrate text content and objects in images. To better the image-text integration, we propose a self-adaptive cross-attention fusion module that helps the image generation to attend more to important text information. Within such a fusion module, we use a self-adaptive learnable factor to learn to flexibly control the influence of cross-attention outputs on image generation. Experimental results show that our method outperforms the state-of-the-art in LTOS, text rendering, and layout-to-image tasks, enabling harmonious visual text rendering and object generation.

KEYWORDS

Diffusion model, Text rendering, Multi-modal generation, Text-object synthesis

1 INTRODUCTION

Controllable text-to-image (T2I) generation [7] synthesizes text contents and objects on an image conditioned on some requirements, which makes the generated images harmoniously juxtaposed with visual text [2] and can be applied to several multi-modal generation scenarios, including emoji crafting [56] and poster design [24]. In particular, text rendering and layout-to-image, as two popular tasks, have appealed to extensive research interests.

Text rendering in images refers to generating clear and legible text in images, which also needs to be visually compatible with the image in terms of texture and depth. This task primarily relies on the LAION5B [54] dataset and its derivatives, where each sample’s input [30] contains a textual description of image layouts and text content with its relation information. Each sample also contains an image as the label (ground truth). Recent text rendering methods typically encode the text input into an image with the backbone of LDMs [52] or ControlNet [72]. TextDiffuser [74] implements a non-end-to-end solution, designing a lightweight character-level text encoder to synthesize text on any given image. GlyphControl [64] leverages glyph conditions instead of character-aware text encoders to render accurate visual text. Recently, AnyText [57] encodes the input with a text embedding layer and an auxiliary latent module, achieving high-quality multi-language text rendering.

Layout-to-image generation task is to generate an image according to a given layout map such as bounding boxes with object categories [31] or a semantic segmentation map [21, 36]. The core of this task is to accurately control the location of generated objects, which can be seen as the reverse task of object detection [78]. It mainly uses datasets including COCO [36] and Flickr30k [65], where the sample’s input contains bounding boxes with assigned object categories [44] and semantic segmentation [42]. GLIGEN [34], standing out as one of the representative models, encodes diverse grounded layout descriptions into new trainable layers through a gated mechanism while freezing the pre-trained LDM, thus achieving text-to-image generation with prompt and bounding box condition inputs.

Despite the impressive progress that has been made in recent research, the majority of these approaches can only accurately control one singular modality: text rendering caters more to the quality of the generated visual text and controls objects simply with prompts, failing to define the positions of the objects elaborately;

layout-to-image generation mainly focuses on accurate control over objects, drawing little attention to the clarity and rationale of the generated visual text. Such differentiation in focus has led to a significant and yet-to-be-bridged gap between the design of methods to control text and objects, although they share similar application scenarios as mentioned.

To mitigate this challenge, we integrate the aforementioned two mainstream tasks - text rendering in images and layout-to-image generation - into a singular task: layout-controllable text-object synthesis (LTOS). The main objective of LTOS is to generate an image with visual text, where the location of the objects and text can be accurately controlled by providing a layout map together with object categories and visual text information. Due to the lack of datasets containing both textual and object layout information to support this task, we developed a layout-aware text-object synthesis dataset, called LTOS dataset. It contains rich well-aligned multi-modal label information including image captions (i.e. prompts in our task), word-level visual text information, and object bounding boxes assigned with the category labels. With Poisson image editing [46], the quality of the images in our dataset is comparable to the real dataset, where the visual text is consistent with the image content in terms of depth, texture, and geometry. Moreover, compared to collecting real data with visual text which is high-cost, our dataset can be easily expanded with a three-step workflow.

Based on our designed dataset, we further propose a layout-controllable text-object adaptive fusion (TOF) framework that synthesizes images with high-quality object and visual text conditioned on the given object layouts and text contents. Our framework consists of 1) an object-layout control module, 2) a visual-text rendering module, and 3) a text-object self-adaptive fusion module. Given the spatial layout information of objects (i.e. object categories with matching bounding boxes), our *object-layout control module* generates images with each object placed at the predetermined location. To render text on the image, our *visual text rendering module* customizes the instructions for rendering text layouts with multi-regional and multi-directional. To harmoniously integrate text content and objects in images, we integrate the above two modules to achieve joint layout control of visual text and objects.

Although integrating the two modules can control text-object multi-modal information, it still struggles with balancing text-object to generate legible visual text on multiple objects. Therefore, we propose a *text-object self-adaptive fusion module* to bridge the visual text rendering and object-layout control via a cross-attention mechanism [59], which fetches important text information to image generation. To flexibly utilize the cross-attention outputs, we further propose a self-adaptive learnable factor that learns to control the influence of cross-attention outputs on image generation. Through the above mechanism, our model can render plausible visual text on diverse objects in multiple regions while maintaining consistency with the texture and geometry of the images. Experimental results on our LTOS dataset show that our method outperforms current state-of-the-art baselines on both text rendering and layout-to-image tasks, indicating the effectiveness of our design. The high-quality generated results also demonstrate that this integrated task and our proposed dataset are of practical application.

Our contributions are fourfold:

- We first merge text rendering and layout-to-image generation tasks and define a single task: layout-controllable text-object synthesis (LTOS) task to harmoniously synthesize text and object into an image.
- We construct a layout-aware text-object synthesis dataset, which includes diverse, elaborate annotations in terms of both object and visual text information, and can be easily expanded through our improved workflow.
- To accomplish the LTOS task, we propose a text-object integration control framework, which customizes the shape and layout of the text and accurately controls the synthesis of text-object multi-modal information.
- We propose a text-object self-adaptive fusion module via adaptive cross-attention mechanisms, effectively bridging text rendering and object generation modules and adaptively using the text-object integrated information.

2 RELATED WORK

2.1 Controllable text-to-image (T2I) generation

Previous controllable T2I approaches can be mainly divided into two groups: autoregressive models [14, 51, 61, 66] and diffusion-based models [34, 43, 50, 52, 58, 63, 70, 76]. Among autoregressive models, Parti [66] treats T2I generation as a sequence-to-sequence modeling problem, with sequences of image tokens as the target outputs, while NÚWA [61], with an adaptive encoder to support different conditions and a novel 3D transformer framework, can edit or generate images and videos for diverse visual synthesis tasks. On the other hand, diffusion-based models are typically built upon diffusion models (DMs) [11] and latent diffusion models (LDMs) [52] that generate images from random noise through a gradual denoising process. Based on class-conditioned diffusion models, GLIDE [43] innovatively replaced the class labels with text, formalizing the first text-to-image diffusion model from high dimension. LDM [52] then realized text-to-image synthesis through its designed attention-based conditioning mechanism during the latent denoising process. Recent research focuses on more accurate and complex text-to-image control [10, 12, 15, 16, 28, 33, 49]. Ge et al. [16] achieved rich-text-to-image generation through a region-based diffusion to enable detailed word-level synthesis. Meanwhile, Ranni [12] injected a semantic panel consisting of detailed control signal parsed by the aid of large language models into the denoising network, thus allowing finely customized generation. While these approaches have propelled the T2I generation to an unprecedented level, it remains a significant limitation that text captions, whether plain or rich, have difficulty conveying accurate layout information for image generation.

2.2 Text rendering in images

Text rendering in images, which aims at integrating legible text into images, is frequently applied in subsequent tasks such as image annotation [20], image synthesis [52], and visual question answering [1]. Early advancements draw inspiration from the analysis in unCLIP [50], and subsequent efforts such as eDiff-I [4]

and Imagen [53] have sought to use the capabilities of large language models, as text encoders in image generation. Recent DeepFloyd IF showed impressive capacity in rendering plausible visual text on images by further improving Imagen [53]. Meanwhile, some approaches [9, 37, 39, 57, 64, 71, 71, 74] tend to improve text rendering capability on existing text-to-image diffusion models [4, 13, 17, 26, 32, 60, 67, 69, 77]. GlyphDraw [39] constructed an image-text dataset with a diffusion-based generator enhanced with glyph and position data to embed text in images coherently, while GlyphControl [64] leveraged pre-rendered glyph images as input condition maps, enabling fine-grained control over the generated glyphs at the layout level. Similarly, TextDiffuser [9] focused on generating layouts from text prompts for more accurate image synthesis by extracting keywords from text prompts. Further AnyText [57] comprises a diffusion pipeline consisting of an auxiliary latent module for generating latent text features from inputs such as glyphs and positions, and a text embedding module that uses OCR for stroke encoding, blending it with image captions to create seamlessly integrated texts. However, current text rendering methods focus mainly on the quality of the visual text, struggling to accurately control the layout of the objects in the generated images.

2.3 Layout-to-Image generation

In contrast to object detection, layout-to-image generation requires the model to generate objects at the corresponding positions providing the bounding boxes and the predetermined category labels. So far various approaches [3, 19, 23, 25, 34, 48, 62, 73, 75] have been introduced to handle this challenge. Initially, Layout2Im [73] applied layout information to help generate images with complex layouts featuring multiple entities. However, the self-attention module used in Layout2Im failed to address the issue of autoregressive repetitive patterns. Meanwhile, GLIGEN [34] used grounded language for its generative process, embedding this information into new trainable layers through a gated mechanism, thus enabling more controlled generation. In addition, SpaText [3] developed a spatial-textual representation through the incorporation of CLIP image embedding, where they stack these object embeddings in the same shapes and positions of the segments to control the layout. LayoutDiffusion [75] proposed to construct a structural image patch with region information and transform the patched image into a special layout to fuse with the normal layout in a unified form to overcome the difficult multi-modal fusion of image and layout. The Spatial-Semantic Map Guided (SSMG) [25] diffusion model adopts the feature map, derived from the layout as guidance, which achieves superior generation quality with sufficient spatial and semantic controllability compared to previous works. Despite the impressive generative capability of these methods, they pay little attention to rendering visual text in images, leading to meaningless and illegible text content.

3 DATASET AND ITS CONSTRUCTIONS

3.1 Dataset Construction

Currently, datasets containing both visual text and object layout information are not readily available. Besides, we notice that datasets [9, 39, 64] that are used for text rendering tasks face some notable limitations: 1) the area of each text region is filtered to be larger

than 10% of the entire image [9, 57]; 2) since existing datasets are mainly designed for generate poster and call-board messages, the visual text typically appears in the center area of the image and rarely in the border area [39]. Therefore, training models with those datasets can lead to potential issues including the incapability to generate 1) tiny-font text and 2) high-quality visual text in border areas.

Considering these limitations, we propose a layout-aware text-object synthesis dataset, a multi-modal dataset containing comprehensive well-aligned labels in terms of both visual text and object information. We choose the Flickr30K [65] dataset as the basis for embedding textual information at appropriate places within images, and the Flickr30K Entities dataset [47] to supplement annotated bounding boxes. Each bounding box is assigned with the corresponding object category label. However, Flickr30K does not include visual text information, which is crucial for our proposed LTOS task. Fortunately, SynthText [18], has provided a potential solution by enriching the data with coarse visual text rendering.

The workflow of dataset construction consists of three steps:

- **Step 1:** Select regions suitable for text rendering by using color or texture and depth information of images;
- **Step 2:** Set filtering rules to generate text as required and color the text based on the Color-model [18] (foreground or background text color model) learned from IIT-5K-word dataset [41];
- **Step 3:** Perform traditional Poisson image editing [46] to blend the text into the scene.

In Particular, the visual text generated in each sample undergoes the following filtering rules in step 2: 1) The number of text regions ranges from [1, 8]; 2) The number of text lines ranges from [1, 8]; 3) The text can be generated in random regions considered suitable for text rendering of the image; 4) Each text region must exceed 2% of the image in length and width, with a minimum area of 5% of the entire image; 5) The text can be randomly rotated, twisted, bolded, and bordered.

While trying to render text based on Flickr30K following this designed workflow, we noticed that the text regions recognized as suitable for text rendering with SynthText were too cluttered, with issues such as underlines and exaggerated shadows in the text style, preventing the results from being used for subsequent tasks. To address the issues, we first replaced the original depth maps by implementing recent Zoedepth [6] to estimate more precise depth and then applied PPOCRv3 [30] to generated data, extracting all text rendered in an image and filtering out all the images whose textual content is not recognizable, i.e. containing low-quality renderings. These optimizations to the workflow enable stable and higher-quality text rendering on images, comparable to the real data in terms of depth, texture, and geometry.

3.2 Dataset Descriptions

Compared to existing text rendering datasets [9, 57], our dataset has the following advantages.

- Existing text rendering datasets typically contain *only one simple object* and the positions of the text regions are mostly confined to the center area since most datasets are designed for generating poster and call-board messages. Our dataset aims to synthesize *multiple objects and visual text with various layouts*.

- The existing datasets collected from the real world may suffer from bias in visual text distribution as the text usually appears on specific objects, such as posters, road signs, and papers. Our dataset is more *diverse on text contents and layouts*, thus having better generalization ability in text rendering. During the construction, we randomly assign text positions and synthesize objects (almost from scratch) instead of using the existing images, which improves the diversity of images.

- Our dataset involves *fine-grained features*: depth of field for fonts, the diverse boldness of the visual text, and word-level bounding boxes information. The features enable the model to capture more details and generate high-fidelity images.

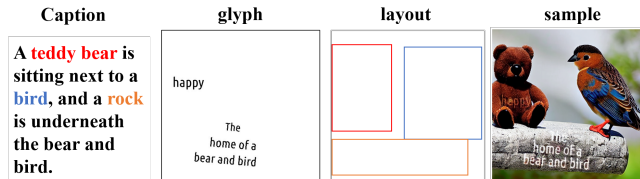


Figure 2: An example sample of our LTOS dataset.

Our proposed LTOS dataset includes 228,973 samples with above 200,000 rendered words in English. Each sample contains (1) an image with rendered text, (2) a caption of the image used as the prompt in our task, (3) grounded word-level text annotations containing enough information to generate the corresponding glyph image, and (4) grounded object annotations [64]. To facilitate subsequent tasks and works, we generate the corresponding glyph image for each sample. Fig. 2 shows an example of our LTOS dataset.

4 METHOD

We first define the LTOS task in Sec. 4.1. Then, we introduce three components of our framework (also shown in Fig. 3). Our framework includes a visual-text control module and an object-layout control module to form the main backbone for text-object integration control (Sec. 4.2). Based on the backbone, we propose a text-object self-adaptive fusion that enables a balanced fusion between text rendering and object generation (Sec. 4.3). Finally, we introduce our training objective in Sec. 4.4.

4.1 Task formulation

For our LTOS task, each sample’s input I is denoted as a triple $I = \langle c, O, G \rangle$, where c represents a prompt, O stands for the object layout map, consisting of object categories and corresponding bounding boxes, and G indicates an explicit glyph image including text content, position, and shape information. Considering the generation of an image containing n objects and m text regions, the corresponding LTOS input instruction can be expressed as:

$$I = \langle c, \{(o_1, b_{o_1}), \dots, (o_n, b_{o_n})\}, \{(t_1, g_{t_1}), \dots, (t_m, g_{t_m})\} \rangle \quad (1)$$

where o_i and t_j denote the object category information and the visual text content respectively, b_{o_i} represents the bounding box information for object o_i , and g_{t_j} is the corresponding glyph region for t_j ($1 \leq i \leq n, 1 \leq j \leq m$).

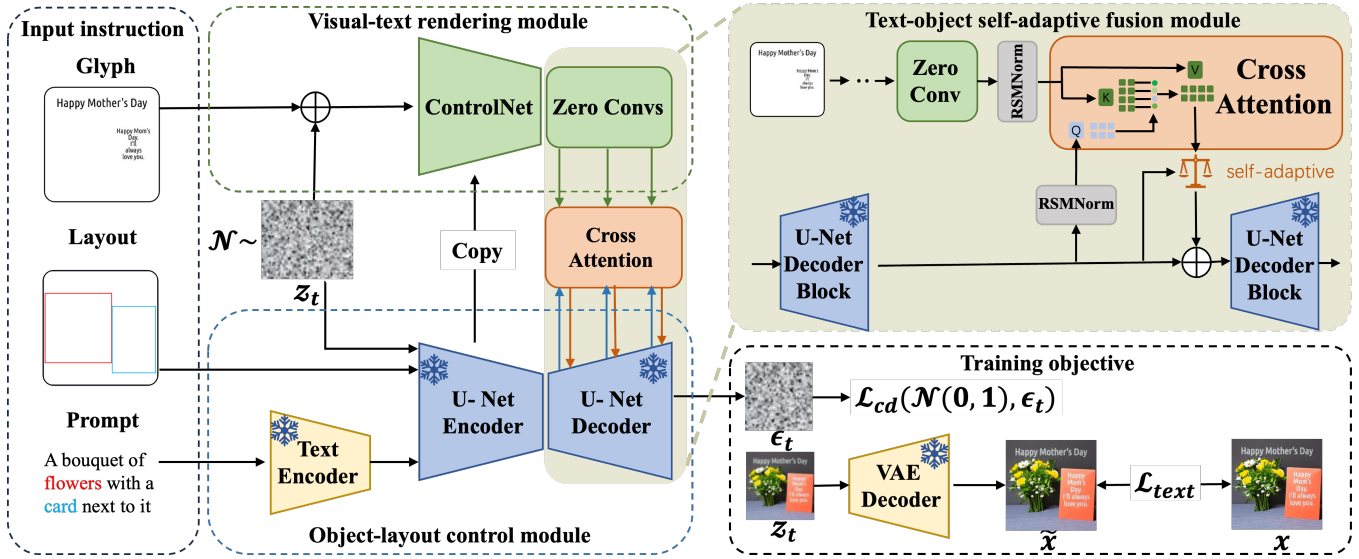


Figure 3: An overview of the proposed TOF method. Taking input instructions consisting of a text prompt, a glyph image, and a layout map, TOF achieves controllable text-object synthesis through multiple components including a visual-text rendering module, an object-layout control module, and a text-object self-adaptive fusion module (the “scale” represents an adaptive learning parameter). The components that are pre-trained and no longer changed are denoted as “frozen”.

Given a predefined or customized LTOS input instruction, the objective is to generate an image that satisfies 1) the generated objects should be within each bounding box, consistent with the specified categories and the text descriptions; 2) the visual text formatting (i.e., position, font size, and distortion) should follow the exact guidance of the glyph image; and 3) the rendered text should be clear, legible and seamlessly integrated with the generated image content in terms of depth, texture, and geometry.

4.2 Text-object integration control model

To handle the aforementioned LTOS task, we first propose an end-to-end framework that combines a visual-text rendering module with an object-layout control module, where the two modules render text content on the image and also generate images with objects conditioned on specific layouts.

Visual-text rendering module. To support customized glyph images and render clear and accurate text in images, we construct a visual-text rendering module focusing on generating visual text with multi-regional and multi-directional layouts. Inspired by Glyph-Control [64] and AnyText [57], we duplicate a trainable ControlNet [72] branch to achieve text rendering for its capability to control the geometric structures accurately. It first takes visual text information including word-level bounding boxes, text content, colors, and fonts as the input. All the information is then consolidated into a glyph image, similar to [64], and is fed into the ControlNet.

Object-layout control module. To generate images accurately according to the given object layout, we build an object layout control module to extract features from the object layout and generate images with the layout. The aforementioned visual-text rendering module can hardly control the accurate layout of the generated

objects, especially in the case of multiple objects, as it is difficult for the model to understand the location information conveyed in the textual guidance or prompt. To control the generation of objects more precisely, our proposed object-layout control module extracts features from the object layout map O based on GLIGEN [34], which enables the open-world synthesis of novel localized concepts by integrating new localization layers. By loading the pre-trained weights, it takes the prompt and the object layout map O as input and can generate objects at the predetermined positions.

Integration control model. With the above two modules enabling controllable visual-text rendering and object generation, it becomes an intuitive idea with a strong motivation to naturally connect the ControlNet-based text rendering branch to the LDM-based object-layout control module, integrating them into a single neural network model. For each LTOS input instruction, the object-layout control module focuses on generating plausible object content according to the layout map. Meanwhile, the text rendering module injects the feature of glyph images as additional conditions to guide the final text-rendered images. While this straightforward combination comprised a seemingly feasible framework for controllable text-object generation, experiments showed that the generated results were not satisfactory and faced certain limitations. To address these issues, we further designed a self-adaptive fusion module.

4.3 Text-object self-adaptive fusion module

To better integrate text and object information (blend text rendering and layout-to-image generation tasks), we propose a text-object self-adaptive fusion module that adaptively bridges the visual-text rendering module and object-layout control module.

The aforementioned text-object integration control module (Sec. 4.2) encountered two notable problems (see Fig. 6 for qualitative examples): (1) it is difficult to reach a balanced training between text rendering and object generation. Over-training the ControlNet branch for text rendering results in the distortion of some generated objects, while under-training makes it difficult to render clear and legible text. (2) when rendering multiple text areas on diverse objects within an image, the visual text in images becomes blurred and unclear. It reflects connection and interaction between the visual-text rendering and object-layout control modules are not yet sufficient, simply through one-way guidance from ControlNet, leaving the training process fragile and preventing the model from handling intricate glyph images as conditions.

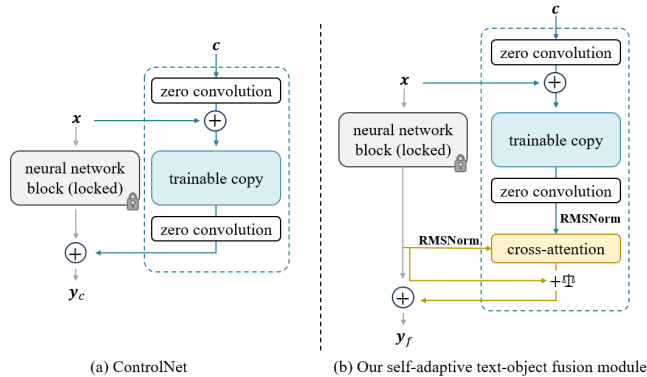


Figure 4: Comparison of ControlNet and our text-object self-adaptive fusion module.

To mitigate this issue, we propose to bridge text and object information via adaptive cross-attention mechanisms, where (1) the cross-attention attends and fetches vital textual information to help image generations, and (2) a self-adaptive learnable factor adaptively learns to leverage the information from the cross-attention. As shown in the middle part of Fig. 4, the adaptive cross-attention transmits textual information from the visual-text rendering module to the hidden layers of the object-layout control module. The adaptive cross-attention consists of three sub-modules as follows.

- **Cross-attention backbone** follows the vanilla cross-attention [45]. As shown in Fig. 4(b), each block B in the object-control module (locked block) corresponds to a trainable copy block with a zero-convolution layer, together denoted as B_z , in the visual-text module. Different from the original ControlNet that directly concatenates the output of B with B_z , we inject an additional cross-attention layer between the output of B and the output of B_z , denoted as y and y_z respectively. The cross-attention layer takes y and y_z as input and output a feature representation y_a that combines the visual text and object information.

- **RMSNorm operation** enables the rapid convergence [68] in our cross-attention backbone. We applied RMSNorm to the input of cross-attention y and y_z (i.e. the output of object-control and zero-convolution). The RMSNorm’s outputs act as the cross-attention’s input as Eq. 2.

$$y_a = \text{cross-attention}(\text{RMSNorm}(y), \text{RMSNorm}(y_z)) \quad (2)$$

- **Self-adaptive learnable factor** learns to decide how much information from cross-attention should be used (determines the influence of cross-attention’s output y_a). It allows the model to adjust the weights of additional visual text information y_a and object information y . We denote the learnable factor as α and apply $\tanh(\alpha)$ to control its range within $[0, 1]$. To linearly weighted integrate y_a and y , as Eq. 3, we element-wise sum up the object information y and y_a adjusted by the factor as α . Then, we concatenate the summation with y^{-1} as the output of this whole module y_f .

$$y_f = \text{concat}(y, y + \tanh(\alpha) * y_a) \quad (3)$$

4.4 Training objective

The training process is as follows: given an input image $x \in \mathbb{R}^{H \times W \times 3}$, we feed the input image into a pre-trained Variational Autoencoder (VAE) [29] to obtain its latent representation $z_0 \in \mathbb{R}^{h \times w \times c}$. In the object-layout control module, the model integrates the objects $\{o_1, \dots, o_n\}$ with the corresponding bounding boxes $\{b_{o_1}, \dots, b_{o_n}\}$ and the image prompt c of x as the input of each gated self-attention layer, denoted as z_b . In the visual-text rendering module, we derive the corresponding glyph image $G = \{g_{t_1}, \dots, g_{t_m}\}$ by processing the visual-text content $\{t_1, \dots, t_m\}$ and the glyph region information $\{g_{t_1}, \dots, g_{t_m}\}$, from which we extract its feature z_g [5, 27]. During the diffusion process, we randomly sample a time $t \sim \text{Uniform}(0, 1000)$ and a Gaussian noise $\epsilon \sim \mathcal{N}(0, 1)$, then corrupt z_0 to generate noisy latent images z_t .

Our training objective consists of two parts: controllable diffusion loss \mathcal{L}_{cd} and text perceptual loss \mathcal{L}_{text} . For \mathcal{L}_{cd} , our model then employs a network ϵ_θ to estimate the noise that has been introduced to the latent image z_t [22], which is optimized as follows:

$$\mathcal{L}_{cd} = \mathbb{E}_{z_0, z_b, z_g, t, \epsilon \sim \mathcal{N}(0, 1)} [\|\epsilon - \epsilon_\theta(z_t, z_b, z_g, t)\|_2^2] \quad (4)$$

To further improve the quality of text rendering, inspired by [57], we incorporate a text perceptual loss \mathcal{L}_{text} to minimize the distance between rendered text in generated image \tilde{x} and the ground truth image x . Specifically, with the help of our grounded word-level text annotations, we crop each x and \tilde{x} pair into sub-images $\mathcal{S} = \{s_1, \dots, s_j\}$ and $\mathcal{S}' = \{s'_1, \dots, s'_j\}$ with one text region in each s_* . We then feed \mathcal{S} and \mathcal{S}' into the PP-OCRv3 model [30] and calculate the mean squared error [8] (MSE) between the extracted features $f_i, f'_i \in \mathbb{R}^{h \times w \times c}$ from the last fully connected layer:

$$\mathcal{L}_{text} = \sum_i \frac{\phi(t)}{hw} \cdot \sum_{h,w} \|f_i - f'_i\|_2^2 \quad (5)$$

where $\phi(t)$ is a weight adjustment function [57] same as the coefficient of diffusion process in [22].

The overall training objective is defined as:

$$\mathcal{L} = \mathcal{L}_{cd} + \lambda * \mathcal{L}_{text} \quad (6)$$

Here, the hyperparameter λ balances the weight between \mathcal{L}_{cd} and \mathcal{L}_{text} , enabling high-quality visual-text rendering without compromising the accuracy of object generation.



Figure 5: Qualitative comparison of TOF and the competitive models. Due to the certain differences between our input instructions and several methods compared, we control the input content to be the same based on the input format accepted by each model, and the specific implementation. Please zoom in to see the details.

5 EXPERIMENT

5.1 Experimental settings

Implementation Details. As introduced in Sec. 4.2, we implement our method based on GLIGEN [34]. Specifically, we loaded the pre-trained “bounding box + text” weight, which is also used to initialize the visual-text rendering module as a “trainable copy” by omitting the gated self-attention layers. We split our proposed dataset into 217,820 training and 11,113 testing samples. For image size, all the input and output images are scaled to 512×512. For the diffusion process, we set the downsampling factor $f = 8$, thus the latent dimension is 64×64×4. We train the model for 130000 iterations with batch size 24 on 3 Tesla A100 GPUs. We use the AdamW [38] optimizer and set the learning rate to 1e-5 for all training. We tested different cross-attention layer settings and reported the results by injecting cross-attention layers between the middle with the first three up-sampling blocks and the corresponding zero-convolution layers of the ControlNet to get the optimal results. During training, the maximum step of the DDPM [22] is set to 1,000, and for inference, we use DDIM [55] with 50 sampling steps. Similar to GLIGEN [34], the prompts and grounding tokens are randomly dropped with a probability of 10% for classifier-free guidance. λ is set to 0.5.

¹We empirically found simple concatenation on y and y_a (without summation of y and y_a) tends to generate blurry and distorted objects.

Baselines. Since LTOS is a novel designed task, we mainly compare our method with the following state-of-the-art baselines: including layout-to-image generation method GLIGEN [34]_{CVPR’22}, based on which we build our model. To evaluate the text rendering quality, we compare our method with TextDiffuser [71]_{NeurIPS’23}, AnyText [57]_{ICLR’24} and GlyphControl [64]_{NeurIPS’23}. For qualitative results, we also compare results from the closed-source model Bing via its official API service.

As the baseline models do not receive exactly the same inputs, to make fair comparisons, we align the inputs of the different models as much as possible. For GLIGEN and Bing, which cannot take the glyph images as input, we extend their text prompts to include the text layout information. For AnyText, which uses text position images instead of glyph images, we blacken the text-render regions of the glyph images as the input.

Metrics. We report three metrics to evaluate the accuracy and quality of both object generation and text rendering: 1) OCR Accuracy (OCR Acc) metric [30], which involves cropping generated text lines based on their specified positions and feeding them to the OCR model for predictions. It calculates the word-level accuracy of the rendered text: each word will be considered correct only if the predicted result exactly matches the ground truth 2) Normalized Edit Distance (NED) [40], which measures the similarity between two strings by quantifying the minimum number of edits required

to transform one string into the other. 3) AP score [35], which reflects the accuracy of object generation. Specifically, we use a pre-trained YOLO-v5s² model to detect bounding boxes on the generated images and compare them with the ground truth boxes using average precision (AP).

5.2 Main results

5.2.1 Quantitative results. The quantitative results are shown in Table 1, where bold results represent the best performance. The results indicate that the clarity and accuracy of the visual text rendered by our method, as measured by OCR, ACC and NED, significantly outperform all state-of-the-art baselines on the benchmark dataset. Our approach outperforms the strongest baseline method TextDiffuser by +18.02% on OCR, ACC and +15.01% on NED. While GlyphControl is retrained on our dataset, it gets relatively low scores. We attribute this to its straightforward use of the ControlNet structure without any balance between object generation and text rendering, which makes it struggle to render high-quality text on multiple objects. It should be noted that GLIGEN’s OCR accuracy and NED score are both close to zero, suggesting that it is unable to generate plausible, legible visual text.

For the layout-to-image generation task, our method achieves comparable results to GLIGEN in terms of the AP score. It indicates that our approach perfectly maintains the capability of accurately generating objects from layout and category information while conducting high-quality visual text rendering. Such improvement demonstrates the advantage and significance of considering both object generation and text rendering simultaneously. It also demonstrates the effectiveness of our designed approach to handle the layout-controllable text-object synthesis task.

5.2.2 Qualitative results. The qualitative results are visualized in Fig. 5. The results show that our method renders more legible, clearer visual texts and plausible objects at the predefined positions. Meanwhile, the text rendered by our approach is more coherent with the image content compared with the baseline models. We conclude that the reason is: on the one hand our model can receive richer information as input to guide the generation; and on the other hand, because the text-object fusion module we have designed enables a more balanced training, allowing the model to focus evenly on both visual-text and object generation, thus it achieves better results.

On the contrary, we observed notable issues and limitations in the baseline models. Although the images generated by AnyText are visually appealing, some images do not contain the desired visual text (the first row) or exhibit errors such as missing, misshapen, and unexpected characters. Results also indicate that they sometimes fail to render text at predefined positions. TextDiffuser and GlyphControl, with glyph images as input, achieve higher-quality visual-text rendering, but there remains inconsistency between visual text and image content they do not perform well with multi-line and multi-region text rendering. Besides, we notice that they fail to render tiny-font text (“wonderful” in the fifth row) and some special characters (“\$” in the sixth row). Furthermore, they sometimes generate objects of the wrong categories or omit some objects. In contrast,

Table 1: The performance of the TOF compared with competing methods. * denotes retraining on our LTOS dataset. We report OCR, ACC, NED, and AP scores.

| Method | OCR, ACC ↑ | NED ↑ | AP ↑ |
|--------------------|---------------|---------------|---------------|
| TextDiffuser [9] | 0.2551 | 0.4824 | - |
| GlyphControl* [64] | 0.1380 | 0.2604 | - |
| AnyText [57] | 0.1732 | 0.3274 | - |
| GLIGEN [34] | 0.0018 | 0.0092 | 0.4958 |
| Ours | 0.4353 | 0.6325 | 0.5658 |

Table 2: Ablation results of TOF on LTOS dataset.

| Cross-Attention | $\mathcal{L}_{\text{text}}$ | α | OCR, ACC ↑ | NED ↑ | AP ↑ |
|-----------------|-----------------------------|----------|---------------|---------------|---------------|
| × | ✓ | × | 0.4114 | 0.6011 | 0.4643 |
| ✓ | ✓ | × | 0.4218 | 0.6177 | 0.4662 |
| ✓ | × | ✓ | 0.4268 | 0.6203 | 0.5003 |
| ✓ | ✓ | ✓ | 0.4353 | 0.6325 | 0.5658 |

our model shows superior generation results in all examples, where both the visual text and the objects meet the requirements.

5.3 Ablation studies

Table 2 verifies the effectiveness of each proposed component. Row 1 and row 4 of Table 2 validate the effectiveness of *text-object self-adaptive fusion*, which is the most crucial component for the LTOS task. The proposed fusion significantly improves the performance by 2.39% in OCR, ACC, 3.14% in NED, and 10.5% in AP, indicating an overall advancement in both text rendering and object generation. We provide qualitative examples in Fig. 6 to show that without this fusion module, the quality of text rendering is not satisfactory. Row 2 in Table 2) ascertains the validity of the *self-adaptive mechanism* in Sec. 4.3. The results indicate that omitting α leads to a decrease in all evaluation metrics (-1.35% in OCR, ACC, -1.48% in NED, and -9.96% in AP). It suggests that the self-adaptive mechanism plays an important role in balancing the generation of visual text and objects. Quantitative results (row 3 in Table 2) show that when we set λ in Eq. 6 to 0, there is a noticeable drop in performance (-0.85% in OCR, ACC, -1.22% in NED, and -6.55% in AP), suggesting that the introduction of *text perceptual loss* further enhances the quality of text generation to a considerable extent.

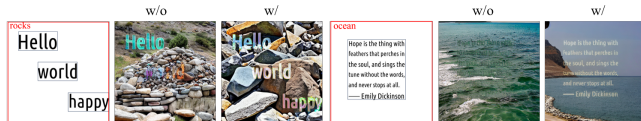


Figure 6: Qualitative results w/o and w/ the text-object self-adaptive fusion module.

²<https://github.com/ultralytics/yolov5>

6 CONCLUSION

In this paper, we explore the challenge of accurately controlling visual text and object generation and provide a detailed analysis and definition of this task, called LTOS. The objective is to generate an image with clear and harmonious visual text, where the location of the objects and text can be precisely controlled. In response to the LTOS task, we propose the LTOS dataset which contains well-aligned multi-modal label information. Furthermore, we propose a novel layout- controllable text-object adaptive fusion framework, called TOF, to handle this challenge. Our approach builds a fundamental pipeline to achieve the simultaneous generation of visual text and objects, then incorporates a text-object self-adaptive fusion module, which balances the rendering of both visual text and object by injecting cross-attention layers. Through extensive experiments, we demonstrate that TOF outperforms the state-of-the-art baselines for text rendering maintaining comparable performance to the object generation model.

REFERENCES

- [1] Stanislaw Antol, Aishwarya Agrawal, Jiasen Lu, Margaret Mitchell, Dhruv Batra, C Lawrence Zitnick, and Devi Parikh. 2015. Vqa: Visual question answering. In *Proceedings of the IEEE/CVF International Conference on Computer Vision*. 2425–2433.
- [2] Loretta Auvil, Eugene Grois, Xavier Llorà, Greg Pape, Vered Goren, Barry Sanders, Bernie Acs, and Robert McGrath. 2007. A flexible system for text analysis with semantic network. *Digital Humanities* (2007), 17–20.
- [3] Omri Avrahami, Thomas Hayes, Oran Gafni, Sonal Gupta, Yaniv Taigman, Devi Parikh, Dani Lischinski, Ohad Fried, and Xi Yin. 2023. Spatext: Spatio-textual representation for controllable image generation. In *Proceedings of the IEEE/CVF Conference on Computer Vision and Pattern Recognition*. 18370–18380.
- [4] Yogesh Balaji, Seungjun Nah, Xun Huang, Arash Vahdat, Jiaming Song, Qingsheng Zhang, Karsten Kreis, Miika Aittala, Timo Aila, Samuli Laine, et al. 2022. ediff-i: Text-to-image diffusion models with an ensemble of expert denoisers. *arXiv preprint arXiv:2211.01324* (2022).
- [5] Arpit Bansal, Hong-Min Chu, Avi Schwarzschild, Soumyadip Sengupta, Micah Goldblum, Jonas Geiping, and Tom Goldstein. 2023. Universal Guidance for Diffusion Models. *arXiv:2302.07121* [cs.CV]
- [6] Shariq Farooq Bhat, Reiner Birkel, Diana Wofk, Peter Wonka, and Matthias Müller. 2023. Zoedepth: Zero-shot transfer by combining relative and metric depth. *arXiv preprint arXiv:2302.12288* (2023).
- [7] Pu Cao, Feng Zhou, Qing Song, and Lu Yang. 2024. Controllable Generation with Text-to-Image Diffusion Models: A Survey. *arXiv preprint arXiv:2403.04279* (2024).
- [8] Tianfeng Chai, Roland R Draxler, et al. 2014. Root mean square error (RMSE) or mean absolute error (MAE). *Geoscientific model development discussions* 7, 1 (2014), 1525–1534.
- [9] Jingye Chen, Yupan Huang, Tengchao Lv, Lei Cui, Qifeng Chen, and Furu Wei. 2024. Textdiffuser: Diffusion models as text painters. *Advances in Neural Information Processing Systems* 36 (2024).
- [10] Ta-Ying Cheng, Matheus Gadelha, Thibault Groueix, Matthew Fisher, Radomir Mech, Andrew Markham, and Niki Trigoni. 2024. Learning Continuous 3D Words for Text-to-Image Generation. *arXiv preprint arXiv:2402.08654* (2024).
- [11] Prafulla Dhariwal and Alexander Nichol. 2021. Diffusion models beat gans on image synthesis. *Advances in Neural Information Processing Systems* 34 (2021), 8780–8794.
- [12] Yutong Feng, Biao Gong, Di Chen, Yujun Shen, Yu Liu, and Jingren Zhou. 2023. Ranni: Taming Text-to-Image Diffusion for Accurate Instruction Following. *arXiv preprint arXiv:2311.17002* (2023).
- [13] Zhida Feng, Zhenyu Zhang, Xintong Yu, Yewei Fang, Lanxin Li, Xuyi Chen, Yuxiang Lu, Jiaxiang Liu, Weichong Yin, Shikun Feng, et al. 2023. Ernie-vilg 2.0: Improving text-to-image diffusion model with knowledge-enhanced mixture-of-denoising-experts. In *Proceedings of the IEEE/CVF Conference on Computer Vision and Pattern Recognition*. 10135–10145.
- [14] Oran Gafni, Adam Polyak, Oran Ashual, Shelly Sheynin, Devi Parikh, and Yaniv Taigman. 2022. Make-a-scene: Scene-based text-to-image generation with human priors. In *European Conference on Computer Vision*. Springer, 89–106.
- [15] Rinon Gal, Yuval Alaluf, Yuval Atzmon, Or Patashnik, Amit H Bermano, Gal Chechik, and Daniel Cohen-Or. 2022. An image is worth one word: Personalizing text-to-image generation using textual inversion. *arXiv preprint arXiv:2208.01618* (2022).
- [16] Songwei Ge, Taesung Park, Jun-Yan Zhu, and Jia-Bin Huang. 2023. Expressive text-to-image generation with rich text. In *Proceedings of the IEEE/CVF International Conference on Computer Vision*. 7545–7556.
- [17] Shuyang Gu, Dong Chen, Jianmin Bao, Fang Wen, Bo Zhang, Dongdong Chen, Lu Yuan, and Baining Guo. 2022. Vector quantized diffusion model for text-to-image synthesis. In *Proceedings of the IEEE/CVF Conference on Computer Vision and Pattern Recognition*. 10696–10706.
- [18] Ankush Gupta, Andrea Vedaldi, and Andrew Zisserman. 2016. Synthetic data for text localisation in natural images. In *Proceedings of the IEEE/CVF Conference on Computer Vision and Pattern Recognition*. 2315–2324.
- [19] Cusuh Ham, James Hays, Jingwan Lu, Krishna Kumar Singh, Zhifei Zhang, and Tobias Hinz. 2023. Modulating pretrained diffusion models for multimodal image synthesis. In *ACM SIGGRAPH 2023 Conference Proceedings*. 1–11.
- [20] Allan Hanbury. 2008. A survey of methods for image annotation. *Journal of Visual Languages & Computing* 19, 5 (2008), 617–627.
- [21] Yutong He, Ruslan Salakhutdinov, and J Zico Kolter. 2023. Localized text-to-image generation for free via cross attention control. *arXiv preprint arXiv:2306.14636* (2023).
- [22] Jonathan Ho, Ajay Jain, and Pieter Abbeel. 2020. Denoising diffusion probabilistic models. *Advances in Neural Information Processing Systems* 33 (2020), 6840–6851.
- [23] Jiun Tian Hoe, Xudong Jiang, Chee Seng Chan, Yap-Peng Tan, and Weipeng Hu. 2024. InteractDiffusion: Interaction Control in Text-to-Image Diffusion Models. In *Proceedings of the IEEE/CVF Conference on Computer Vision and Pattern Recognition*.
- [24] Huiyu Huo, Feng Wang, et al. 2022. A study of artificial intelligence-based poster layout design in visual communication. *Scientific Programming* 2022 (2022).
- [25] Chengyou Jia, Minnan Luo, Zhuohang Dang, Guang Dai, Xiaojun Chang, Mengmeng Wang, and Jingdong Wang. 2024. Ssmg: Spatial-semantic map guided diffusion model for free-form layout-to-image generation. In *Proceedings of the AAAI Conference on Artificial Intelligence*, Vol. 38. 2480–2488.
- [26] Chao Jia, Yinfei Yang, Ye Xia, Yi-Ting Chen, Zarana Parekh, Hieu Pham, Quoc Le, Yun-Hsuan Sung, Zhen Li, and Tom Duerig. 2021. Scaling up visual and vision-language representation learning with noisy text supervision. In *International conference on machine learning*. PMLR, 4904–4916.
- [27] Sungyun Kim, Junsoo Lee, Kibeom Hong, Daesik Kim, and Namhyuk Ahn. 2023. DiffBlender: Scalable and Composable Multimodal Text-to-Image Diffusion Models. *arXiv:2305.15194* [cs.CV]
- [28] Yunji Kim, Jiyoung Lee, Jin-Hwa Kim, Jung-Woo Ha, and Jun-Yan Zhu. 2023. Dense Text-to-Image Generation with Attention Modulation. *arXiv:2308.12964* [cs.CV]
- [29] Diederik P Kingma and Max Welling. 2013. Auto-encoding variational bayes. *arXiv preprint arXiv:1312.6114* (2013).
- [30] Chenxia Li, Weiwei Liu, Ruoyu Guo, Xiaoting Yin, Kaitao Jiang, Yongkun Du, Yuning Du, Lingfeng Zhu, Baohua Lai, Xiaoguang Hu, et al. 2022. PP-OCRv3: More attempts for the improvement of ultra lightweight OCR system. *arXiv preprint arXiv:2206.03001* (2022).
- [31] Liunan Harold Li, Pengchuan Zhang, Haotian Zhang, Jianwei Yang, Chunyuan Li, Yiyu Zhong, Lijuan Wang, Lu Yuan, Lei Zhang, Jenq-Neng Hwang, et al. 2022. Grounded language-image pre-training. In *Proceedings of the IEEE/CVF Conference on Computer Vision and Pattern Recognition*. 10965–10975.
- [32] Wei Li, Xue Xu, Xinyan Xiao, Jiachen Liu, Hu Yang, Guohao Li, Zhanpeng Wang, Zhifan Feng, Qiaoqiao She, Yajuan Lyu, et al. 2022. Upainting: Unified text-to-image diffusion generation with cross-modal guidance. *arXiv preprint arXiv:2210.16031* (2022).
- [33] Yuheng Li, Haotian Liu, Yangming Wen, and Yong Jae Lee. 2023. Generate Anything Anywhere in Any Scene. *arXiv:2306.17154* [cs.CV]
- [34] Yuheng Li, Haotian Liu, Qingyang Wu, Fangzhou Mu, Jianwei Yang, Jianfeng Gao, Chunyuan Li, and Yong Jae Lee. 2023. Gligen: Open-set grounded text-to-image generation. In *Proceedings of the IEEE/CVF Conference on Computer Vision and Pattern Recognition*. 22511–22521.
- [35] Zejian Li, Jingyu Wu, Immanuel Koh, Yongchuan Tang, and Lingyun Sun. 2021. Image synthesis from layout with locality-aware mask adaption. In *Proceedings of the IEEE/CVF International Conference on Computer Vision*. 13819–13828.
- [36] Tsung-Yi Lin, Michael Maire, Serge Belongie, James Hays, Pietro Perona, Deva Ramanan, Piotr Dollár, and C Lawrence Zitnick. 2014. Microsoft coco: Common objects in context. In *Computer Vision—ECCV 2014: 13th European Conference, Zurich, Switzerland, September 6–12, 2014, Proceedings, Part V* 13. Springer, 740–755.
- [37] Rosanne Liu, Dan Garrette, Chitwan Saharia, William Chan, Adam Roberts, Sharan Narang, Irina Blok, RJ Mical, Mohammad Norouzi, and Noah Constant. 2022. Character-aware models improve visual text rendering. *arXiv preprint arXiv:2212.10562* (2022).
- [38] Ilya Loshchilov and Frank Hutter. 2017. Decoupled weight decay regularization. *arXiv preprint arXiv:1711.05101* (2017).
- [39] Jian Ma, Mingjun Zhao, Chen Chen, Ruichen Wang, Di Niu, Haonan Lu, and Xiaodong Lin. 2023. Glyphdraw: Learning to draw chinese characters in image synthesis models coherently. *arXiv preprint arXiv:2303.17870* (2023).

- [40] E. Marzal, A.;Vidal. 1993. Computation of normalized edit distance and applications. *Pattern Analysis and Machine Intelligence, IEEE Transactions on* (1993), 926–932. Issue NO.9.
- [41] A. Mishra, K. Alahari, and C. V. Jawahar. 2012. Scene Text Recognition using Higher Order Language Priors. In *BMVC*.
- [42] Yujian Mo, Yan Wu, Xinneng Yang, Feilin Liu, and Yujun Liao. 2022. Review the state-of-the-art technologies of semantic segmentation based on deep learning. *Neurocomputing* 493 (2022), 626–646.
- [43] Alex Nichol, Prafulla Dhariwal, Aditya Ramesh, Pranav Shyam, Pamela Mishkin, Bob McGrew, Ilya Sutskever, and Mark Chen. 2021. Glide: Towards photorealistic image generation and editing with text-guided diffusion models. *arXiv preprint arXiv:2112.10741* (2021).
- [44] Constantine P Papageorgiou, Michael Oren, and Tomaso Poggio. 1998. A General Framework for Object Detection. In *Proceedings of the IEEE/CVF International Conference on Computer Vision*. 555.
- [45] Ashish Vaswani;Noam Shazeer;Niki Parmar. 2017. Attention is all you need. In *Proceedings of the International Conference on Neural Information Processing Systems*.
- [46] Patrick Pérez, Michel Gangnet, and Andrew Blake. 2023. Poisson image editing. In *Seminal Graphics Papers: Pushing the Boundaries, Volume 2*. 577–582.
- [47] Bryan A. Plummer, Liwei Wang, Christopher M. Cervantes, Juan C. Caicedo, Julia Hockenmaier, and Svetlana Lazebnik. 2017. Flickr30K Entities: Collecting Region-to-Phrase Correspondences for Richer Image-to-Sentence Models. *IJCV* 123, 1 (2017), 74–93.
- [48] Zipeng Qi, Guoxi Huang, Zebin Huang, Qin Guo, Jinwen Chen, Junyu Han, Jian Wang, Gang Zhang, Lufei Liu, Errui Ding, et al. 2023. Layered Rendering Diffusion Model for Zero-Shot Guided Image Synthesis. *arXiv preprint arXiv:2311.18435* (2023).
- [49] Leigang Qu, Wenjie Wang, Yongqi Li, Hanwang Zhang, Liqiang Nie, and Tat-Seng Chua. 2024. Discriminative Probing and Tuning for Text-to-Image Generation. *arXiv preprint arXiv:2403.04321* (2024).
- [50] Aditya Ramesh, Prafulla Dhariwal, Alex Nichol, Casey Chu, and Mark Chen. 2022. Hierarchical text-conditional image generation with clip latents. *arXiv preprint arXiv:2204.06125* 1, 2 (2022), 3.
- [51] Aditya Ramesh, Mikhail Pavlov, Gabriel Goh, Scott Gray, Chelsea Voss, Alec Radford, Mark Chen, and Ilya Sutskever. 2021. Zero-shot text-to-image generation. In *International conference on machine learning*. Pmlr, 8821–8831.
- [52] Robin Rombach, Andreas Blattmann, Dominik Lorenz, Patrick Esser, and Björn Ommer. 2022. High-resolution image synthesis with latent diffusion models. In *Proceedings of the IEEE/CVF Conference on Computer Vision and Pattern Recognition*. 10684–10695.
- [53] Chitwan Saharia, William Chan, Saurabh Saxena, Lala Li, Jay Whang, Emily L Denton, Kamyar Ghasemipour, Raphael Gontijo Lopes, Burcu Karagol Ayan, Tim Salimans, et al. 2022. Photorealistic text-to-image diffusion models with deep language understanding. *Advances in Neural Information Processing Systems* 35 (2022), 36479–36494.
- [54] Christoph Schuhmann, Romain Beaumont, Richard Vencu, Cade Gordon, Ross Wightman, Mehdi Cherti, Theo Coombes, Aarush Katta, Clayton Mullis, Mitchell Wortsman, et al. 2022. Laion-5b: An open large-scale dataset for training next generation image-text models. *Advances in Neural Information Processing Systems* 35 (2022).
- [55] Jiaming Song, Chenlin Meng, and Stefano Ermon. 2020. Denoising diffusion implicit models. *arXiv preprint arXiv:2010.02502* (2020).
- [56] Chaitanya Krishna Suryadevara. 2019. EMOJIFY: CRAFTING PERSONALIZED EMOJIS USING DEEP LEARNING. *International Journal of Innovations in Engineering Research and Technology* 6, 12 (2019), 49–56.
- [57] Yuxiang Tuo, Wangmeng Xiang, Jun-Yan He, Yifeng Geng, and Xuansong Xie. 2023. AnyText: Multilingual Visual Text Generation and Editing. In *The Twelfth International Conference on Learning Representations*.
- [58] Anwaar Ulhaq and Naveed Akhtar. 2024. Efficient Diffusion Models for Vision: A Survey. *arXiv:2210.09292* [cs.CV]
- [59] Ashish Vaswani, Noam Shazeer, Niki Parmar, Jakob Uszkoreit, Llion Jones, Aidan N Gomez, Łukasz Kaiser, and Illia Polosukhin. 2017. Attention is all you need. *Advances in Neural Information Processing Systems* 30 (2017).
- [60] Zihao Wang, Wei Liu, Qian He, Xinglong Wu, and Zili Yi. 2022. Clip-gen: Language-free training of a text-to-image generator with clip. *arXiv preprint arXiv:2203.00386* (2022).
- [61] Chenfei Wu, Jian Liang, Lei Ji, Fan Yang, Yuejian Fang, Daxin Jiang, and Nan Duan. 2022. Nūwa: Visual synthesis pre-training for neural visual world creation. In *European conference on computer vision*. Springer, 720–736.
- [62] Han Xue, Zhiwu Huang, Qianru Sun, Li Song, and Wenjun Zhang. 2023. Freestyle layout-to-image synthesis. In *Proceedings of the IEEE/CVF Conference on Computer Vision and Pattern Recognition*. 14256–14266.
- [63] Ling Yang, Zhilong Zhang, Yang Song, Shenda Hong, Runsheng Xu, Yue Zhao, Wentao Zhang, Bin Cui, and Ming-Hsuan Yang. 2024. Diffusion Models: A Comprehensive Survey of Methods and Applications. *arXiv:2209.00796* [cs.LG]
- [64] Yukang Yang, Dongnan Gui, Yuhui Yuan, Weicong Liang, Haisong Ding, Han Hu, and Kai Chen. 2024. GlyphControl: Glyph Conditional Control for Visual Text Generation. *Advances in Neural Information Processing Systems* 36 (2024).
- [65] Peter Young, Alice Lai, Micah Hodosh, and Julia Hockenmaier. 2014. From image descriptions to visual denotations: New similarity metrics for semantic inference over event descriptions. *TACL* 2 (2014), 67–78.
- [66] Jiahui Yu, Yuanzhong Xu, Jing Yu Koh, Thang Luong, Gunjan Baid, Zirui Wang, Vijay Vasudevan, Alexander Ku, Yinfei Yang, Burcu Karagol Ayan, et al. 2022. Scaling autoregressive models for content-rich text-to-image generation. *arXiv preprint arXiv:2206.10789* 2, 3 (2022), 5.
- [67] Lu Yuan, Dongdong Chen, Yi-Ling Chen, Noel Codella, Xiyang Dai, Jianfeng Gao, Houdong Hu, Xuedong Huang, Boxin Li, Chunyuan Li, et al. 2021. Florence: A new foundation model for computer vision. *arXiv preprint arXiv:2111.11432* (2021).
- [68] Biao Zhang and Rico Sennrich. 2019. Root mean square layer normalization. *Advances in Neural Information Processing Systems* 32 (2019).
- [69] Chenshuang Zhang, Chaoning Zhang, Mengchun Zhang, and In So Kweon. 2023. Text-to-image diffusion model in generative ai: A survey. *arXiv preprint arXiv:2303.07909* (2023).
- [70] Chenshuang Zhang, Chaoning Zhang, Mengchun Zhang, and In So Kweon. 2023. Text-to-image Diffusion Models in Generative AI: A Survey. *arXiv:2303.07909* [cs.CV]
- [71] Lingjun Zhang, Xinyuan Chen, Yaohui Wang, Yue Lu, and Yu Qiao. 2024. Brush your text: Synthesize any scene text on images via diffusion model. In *Proceedings of the AAAI Conference on Artificial Intelligence*. Vol. 38. 7215–7223.
- [72] Lvmin Zhang, Anyi Rao, and Maneesh Agrawala. 2023. Adding conditional control to text-to-image diffusion models. In *Proceedings of the IEEE/CVF International Conference on Computer Vision*. 3836–3847.
- [73] Bo Zhao, Lili Meng, Weidong Yin, and Leonid Sigal. 2019. Image generation from layout. In *Proceedings of the IEEE/CVF Conference on Computer Vision and Pattern Recognition*. 8584–8593.
- [74] Yiming Zhao and Zhouhui Lian. 2023. UDiffText: A Unified Framework for High-quality Text Synthesis in Arbitrary Images via Character-aware Diffusion Models. *arXiv preprint arXiv:2312.04884* (2023).
- [75] Guangcong Zheng, Xianpan Zhou, Xuwei Li, Zhongang Qi, Ying Shan, and Xi Li. 2023. Layoutdiffusion: Controllable diffusion model for layout-to-image generation. In *Proceedings of the IEEE/CVF Conference on Computer Vision and Pattern Recognition*. 22490–22499.
- [76] Yufan Zhou, Bingchen Liu, Yizhe Zhu, Xiao Yang, Changyou Chen, and Jinhui Xu. 2023. Shifted diffusion for text-to-image generation. In *Proceedings of the IEEE/CVF Conference on Computer Vision and Pattern Recognition*. 10157–10166.
- [77] Yufan Zhou, Ruiyi Zhang, Changyou Chen, Chunyuan Li, Chris Tensmeyer, Tong Yu, Jiuxiang Gu, Jinhui Xu, and Tong Sun. 2022. Towards language-free training for text-to-image generation. In *Proceedings of the IEEE/CVF Conference on Computer Vision and Pattern Recognition*. 17907–17917.
- [78] Zhengxia Zou, Keyan Chen, Zhenwei Shi, Yuhong Guo, and Jieping Ye. 2023. Object detection in 20 years: A survey. *Proc. IEEE* 111, 3 (2023), 257–276.